# Mass transfer enhancement factor for chemical absorption of carbon dioxide into sodium metaborate solution

**Duygu Uysal Zıraman[†], Özkan Murat Doğan, and Bekir Zühtü Uysal**

Department of Chemical Engineering and Clean Energy Research and Application Center (CERAC-TEMENAR),
Gazi University, Maltepe, Ankara, 06570, Turkey

**Abstract**–Hydrogen is getting increasing attention as a medium for energy storage, and sodium borohydride is accepted as a suitable carrier for hydrogen. The main product of the process by means of which hydrogen is produced from sodium borohydride is sodium metaborate. Our aim was to find an alternative use for sodium metaborate and specifically investigating the feasibility to use it for carbon dioxide capture from flue gases. The products of this chemical absorption are sodium carbonate, sodium bicarbonate and boric acid, all of which are industrially important chemicals. A bubble column was used in the experiments. Oxygen desorption technique was employed to determine the liquid side physical mass transfer coefficient. Chemical mass transfer coefficient was determined by absorption of carbon dioxide from its mixture with nitrogen into sodium metaborate solution. Enhancement factor was then calculated and a correlation was developed for it.

Keywords: Carbon Dioxide Absorption with Chemical Reaction, Sodium Metaborate, Bubble Column, Mass Transfer, Enhancement Factor

## INTRODUCTION

It is strongly believed that hydrogen will be the energy carrier in the near future, and sodium borohydride is one of the best hydrogen carriers. Current problem in this technology is, however, either to recycle or to find alternative use for sodium metaborate, which is the product of the process by means of which hydrogen is obtained from sodium borohydride.

Besides this, carbon dioxide ($CO_2$) is one of the major greenhouse gases and it is seen as the primary cause for global warming. The removal of $CO_2$ as well as other acidic gases such as $H_2S$, $SO_2$ and COS from flue gas in fossil fueled power generation is an important operation for the abatement of greenhouse gas emissions. This process, simply called post combustion carbon dioxide capture process, has attracted substantial attention as it also allows retrofitting in existing power plants. Alkanolamines, such as monoethanol amine (MEA), diethanol amine (DEA), di-isopropanol amine (DIPA) and methyldiethanol amine (MDEA), have been the mostly employed solvents in this process [1-6], with MEA the most common one. It is also common practice to add some additives to promote the rate of absorption [7-9]. Degradation in time, corrosive properties and large energy requirement for desorption of $CO_2$ in a cyclic process using alkanolamines have made it necessary to look for alternative solvents [10,11]. The use of, for example, aqueous ammonia solution has evolved in this effort [12-17]. Though, the necessity to work relatively at low temperatures (0-10 °C) for $CO_2$ absorption by ammonia process seems to be another important drawback. Thus, investigations will continue to come up with an appropriate solvent enabling efficient absorption of $CO_2$ at operating conditions close to atmospheric conditions.

In this work, sodium metaborate was used to capture $CO_2$. Therefore, it serves both objectives: to capture carbon dioxide emission from combustion of fossil fuels and to help finding alternative areas of use for sodium metaborate. The products of this chemical absorption are sodium carbonate, sodium bicarbonate and boric acid; all are individually important chemicals in industry and in fact can be used directly as a mixture, for example, in glass industry. The present work was planned with the hope of contribution to the use of hydrogen energy as well by utilizing the product of sodium borohydride hydration reaction [18].

In addition, scientific and industrial interest in bubble columns has increased considerably in the last decades [19-21]. A bubble column is simple, easy to operate, control and scale up, and effective in contacting gas and liquid streams [22,23]. High interfacial areas as a few thousand $m^2/m^3$ can be achieved with porous plate spargers [24]. Its simplicity and effectiveness were the primary reasons of its use as a contactor in the present work.

The capability of sodium metaborate to absorb carbon dioxide and the kinetics of the reaction between dissolved carbon dioxide and the sodium metaborate were investigated previously [18]. In this work, chemical absorption studies were performed with a bubble column operating continuously with respect to liquid and gas to see the extent of enhancement factor attainable for carbon dioxide capture by sodium metaborate with respect to physical absorption.

## THEORETICAL BACKGROUND AND EXPERIMENTAL

To investigate the absorption of carbon dioxide into sodium

---

[†]To whom correspondence should be addressed.
E-mail: duysal@gazi.edu.tr

metaborate solution, work was performed by using a bubble column, a widely used liquid-gas contactor. Bubble columns are one of the multiphase systems. Their ratio of height to diameter is generally within the range of 1.5-20 [25]. A bubble column is simply considered as a tank with a gas distributor at the bottom. Their heat and mass transfer characteristics are excellent, meaning they provide high coefficients of heat and mass transfer. They do not have mobile pieces in the system and are compact, so maintenance and operating costs are low [26].

The characterization of fluid dynamics of bubble columns is very important for operation and performance of the system. It is highly dependent on the flow regime attained. The classification of the flow regime is done according to the gas flow rate [21]. There are mainly three type of flow regimes: homogeneous (bubbly flow), heterogeneous (churn-turbulent flow) and slug [27]. There are also regions between the main regimes, known as the transition ranges. It is not possible to give certain gas flow rate intervals for all these regimes. There are many studies done in different systems and the results of intervals for these regimes and regime boundaries are different from each other [21,27-31]. These qualifications are specific properties of a column; hence, first, flow characteristics should be identified in a study using a bubble column. The main characteristic property affecting the performance is the gas holdup. So this work was planned to determine the gas holdup first and then to investigate the mass transfer aspect. Since the $CO_2$ absorption is with chemical reaction, studies for the calculation of both physical and chemical mass transfer coefficients were done to see the enhancement due to chemical reaction [18]. Liquid side physical mass transfer coefficient was determined employing oxygen desorption method. Chemical mass transfer coefficient was determined by wet analysis method. The enhancement factor was then calculated to see the contribution of the reaction to absorption.

The reactions taking place in the process of carbon dioxide absorption into sodium metaborate solution are given below [18].

$$2H_2O \leftrightarrow 2H^+ + 2OH^- \tag{1}$$

$$2NaBO_2 \rightarrow 2Na^+ + 2BO_2^- \tag{2}$$

$$CO_2(g) \rightarrow CO_2(l) \tag{3}$$

$$CO_2(l) + OH^- \leftrightarrow HCO_3^- \tag{4}$$

$$HCO_3^- + OH^- \leftrightarrow CO_3^= + H_2O \tag{5}$$

$$2Na^+ + CO_3^= \rightarrow Na_2CO_3 \tag{6}$$

$$2H_2O + 2H^+ + 2BO_2^- \rightarrow 2H_3BO_3 \tag{7}$$

According to this mechanism, the water molecules dissociate, and sodium and metaborate ions are dispersed in water. Carbon dioxide gas passing to the solution first dissolves in this solution and forms bicarbonate and carbonate ions with hydroxide ions of dissociated water. These ions immediately proceed to react with sodium ions, producing eventually sodium carbonate. The other ions, which are hydrogen ions of dissociated water and borate ions, produce boric acid.

Note that the anion present in aqueous solutions of metaborates is the tetrahedral monoborate ion, which is $B(OH)_4^-$ [32,33], but due to simplicity, the $B(OH)_4^-$ ion can be abbreviated and written
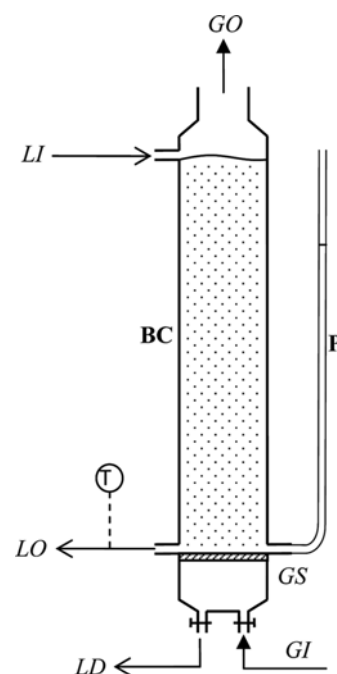


**Fig. 1. Bubble column.**
**BC**. Bubble column
GI. Gas inlet from humidifier (15% $CO_2$-85% Air mixture saturated with water vapor)
GO. Gas outlet
LD. Liquid drainage outlet of bubble column
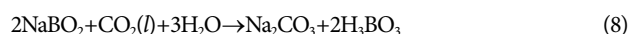LI. Liquid inlet from tank by a peristaltic pump
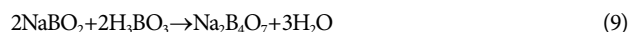LO. Liquid outlet to (sodium metaborate) tank
GS. Gas sparger
**P**. Piezometer

as $BO_2^-$ [33].

The overall reaction between dissolved carbon dioxide and sodium metaborate can then be written as follows:

$$2NaBO_2 + CO_2(l) + 3H_2O \rightarrow Na_2CO_3 + 2H_3BO_3 \tag{8}$$

Excess sodium metaborate also reacts with boric acid to give borax [18].

$$2NaBO_2 + 2H_3BO_3 \rightarrow Na_2B_4O_7 + 3H_2O \tag{9}$$

## 1. Experimental Setup

The experimental setup is shown in Fig. 1. A Pyrex column with a diameter of 80 mm and a height of 750 mm was used in the experiments. The solution was prepared in 50 L tank and fed to the top of the column by a calibrated pump (Heidolph Pumpdrive 5206 with Masterflex pump pipe 96410-14). Air or $CO_2$-air mixture was first passed through a humidifier to saturate it with water and then introduced to the porous glass sparger at the bottom of the column. The gas flow rate was measured by a Cole-Parmer rotameter. Gas and liquid flow rates were chosen to ensure smooth bubbly flow [34]. The liquid flow rate was varied between 0.5-1.8 L/min and the gas between 4-40 L/min.

## 2. Gas Holdup Measurement

Holdup was determined by measuring the liquid height in the piezometer and in the column, as shown in Fig. 1. By the equations given below, liquid and gas holdups of the column at different rates of gas ranging between 4-40 L/min were calculated.

$$\varepsilon_L = \frac{H_{piezometer}}{H_{column}} \tag{10}$$

$$\varepsilon_G = \frac{H_{column} - H_{piezometer}}{H_{column}} = 1 - \varepsilon_L \tag{11}$$

## 3. Liquid Side Physical Mass Transfer Coefficient

Liquid side physical mass transfer coefficient was determined employing oxygen desorption method. Distilled water saturated with oxygen in an external tank was fed to the column where it was brought in contact in a countercurrent mode with rising bubbles of air. The concentration of oxygen in water at the inlet and at the exit of the column was measured using an oxygen meter (YSI Incorporated Model 50B Dissolved Oxygen Meter). The superficial velocities of air and liquid were changed between 0.0185-0.1 m/s and 0.0017-0.0068 m/s, respectively. Liquid side physical mass transfer coefficient for oxygen was calculated using the following expression;

$$(k_x^o a) = \frac{L}{z_T s_c} \ln\left(\frac{x_{in} - x_i}{x_{out} - x_i}\right) \tag{12}$$

Here, $x_i$ is the interfacial composition at the liquid side in equilibrium with the gas side oxygen composition. It can be assumed to be constant for the temperature at which the experiment was carried out. These values can be found in the literature [35] as a function of temperature and should be corrected for the total pressure.

Physical mass transfer coefficient, $k_L^0 a$, can be calculated as follows:

$$(k_L^0 a) = \frac{(k_x^0 a)}{c} \tag{13}$$

where c is the total concentration at the liquid side. Since $k_L^0 a$ is proportional to the square root of the diffusivity, liquid side physical mass transfer coefficient for carbon dioxide can be estimated using the following correction factor [35,36]:

$$\frac{(k_L^0 a)_{CO_2}}{(k_L^0 a)_{O_2}} = \sqrt{\frac{D_{CO_2}^{H_2O}}{D_{O_2}^{H_2O}}} = 0.807 \tag{14}$$

## 4. Liquid Side Chemical Mass Transfer Coefficient

Liquid side mass transfer coefficient for absorption of carbon dioxide with chemical reaction was determined by performing experiments where carbon dioxide was absorbed into sodium metaborate solution in the column operating in the countercurrent mode with continuous gas and liquid phases. The gas phase fed to the column consisted of 15 mol% $CO_2$ and 85 mol% $N_2$. This is a typical maximum possible value of $CO_2$ in the flue gas of coal combustion systems in industry. The liquid feed was 4.5 wt-% sodium metaborate solution. The reason for using concentrated solution was to neglect the change in the solution properties during absorption.

Considering the reaction between carbon dioxide and sodium metaborate given above, wet chemical analysis of the liquid at the inlet and exit for carbonates enabled the calculation of the total rate of carbon dioxide absorption, W [mol/s]. This can also be expressed in terms of average mass flux, $N_{CO_2}$.

$$W\left[\frac{mol}{s}\right] = N_{CO_2}\left[\frac{mol}{m^2 s}\right] a\left[\frac{m^2}{m^3}\right](S_C Z_t)[m^3] \tag{15}$$

Noting,

$$S_C Z_t = V \tag{16}$$

The average mass flux, $N_{CO_2}$, becomes;

$$N_{CO_2} a = W/V \tag{17}$$

and using the definition of the flux, volumetric mass transfer coefficient for $CO_2$ with fast chemical reaction can be estimated.

$$k_x(x_i - x_{bulk})a = k_x(x_i - 0)a = W/V \tag{18}$$

or,

$$(k_x a) = W/(V \cdot x_i) \tag{19}$$

This can easily be converted to chemical mass transfer coefficient, $k_L a$;

$$k_L a = \frac{k_x a}{c} \tag{20}$$

## 5. Enhancement Factor

The enhancement factor, which is a measure of the contribution of chemical reaction to the absorption process, is represented by the ratio of the rate of absorption with chemical reaction to the rate of physical absorption. Using the definition of the mass transfer flux, the experimental value of the enhancement factor for chemical absorption of carbon dioxide can be expressed as follows:

$$E = \frac{k_L a}{k_L^0 a} \tag{21}$$

where, $k_L a$ is the chemical mass transfer coefficient and $k_L^0 a$ is the physical mass transfer coefficient.

## RESULTS AND DISCUSSION

## 1. Gas Holdup

The overall mass transfer rate per unit volume in a bubble column is mostly governed by the liquid-side mass transfer coefficient [37]. Moreover, in a bubble column the variation of the overall mass transfer coefficient per unit volume is primarily due to variations in the interfacial area [38]. Thus, precise knowledge of gas holdup is needed to determine the performance of bubble columns. The basic factors affecting gas holdup are superficial gas velocity, liquid properties, column dimensions, operating temperature and pressure and gas distributor design [21]. It is recommended to consider the flow regime map for bubble columns to identify the regime involved before adapting any correlation [34,39]. Even for similar studies at comparable gas velocities, gas holdup values reported may show differences of more than two-fold [21]. The best approach is, therefore, to determine the gas holdup experimentally for the column in which mass transfer studies are carried out. Gas holdup, determined from piezometer readings, with increasing and decreasing gas velocities is given in Fig. 2.

Note that the present data values are close to the predictions made by the correlation of Joshi and Sharma [40] at low gas velocities and to those of Kawase and Moo-Young [41] at high gas velocities. Considering the column diameter and gas velocities employed in the present research, the flow regime in the present study starts with
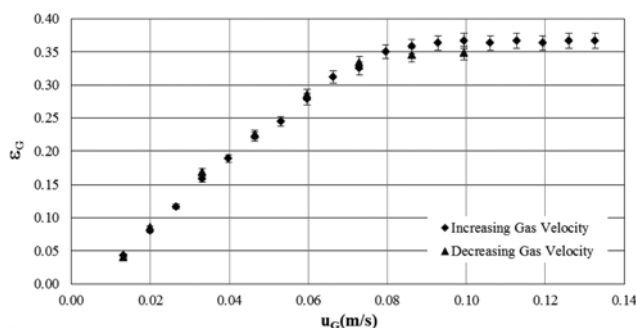
Fig. 2. Variation of gas holdup with the gas velocity (with 3% error bars).

homogeneous bubble flow at low velocities up to about 0.035 m/s and then falls mostly in the transition regime [34]. At velocities greater than about 0.08 m/s the regime becomes slug flow and the gas holdup does not show appreciable variation. The variation of gas holdup values in the present study thus indicate clearly the change from homogeneous bubble flow to transition regime, covering both ranges, and implying the passage from Joshi and Sharma correlation predictions at low gas velocities to Kawase and Moo Young correlation predictions at relatively high gas velocities. As gas holdup may also be affected by the wall effects for column diameters smaller than 0.1 m and the sparger design employed [34,42], it was preferred to develop a correlation for the present work. The correlation developed was in a form similar to that of Joshi and Sharma [40] due to its simplicity and is given below ($r^2$=0.99):

$$\varepsilon_G = \frac{15.14u_G}{3.18 + 2u_G} \tag{22}$$

## 2. Liquid Side Physical Mass Transfer Coefficient

The data obtained from the experiments for desorption of oxygen and Eqs. (12), (13) and (14) were used to calculate the liquid side physical volumetric mass transfer coefficient for carbon dioxide. The results are given in Fig. 3. The values of $k_L^0 a$ are in good
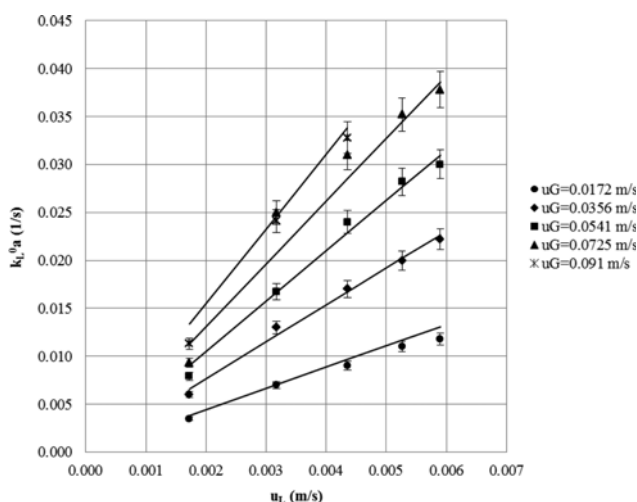


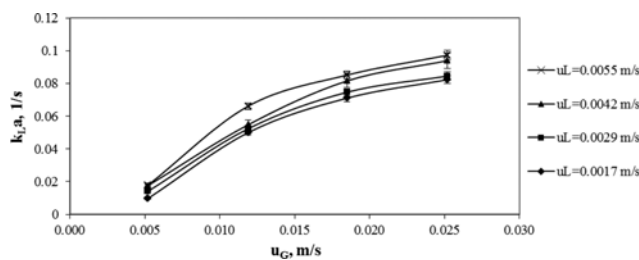Fig. 3. Liquid side volumetric physical mass transfer coefficient for carbon dioxide (with 5% error bars).



Fig. 4. Liquid side mass transfer coefficient with chemical reaction (with 3% error bars).

agreement with the literature [43]. These results were subjected to a regression analysis and the following correlation was developed with $r^2$=0.92.

$$(k_L^0 a)_{CO_2} = 46.84u_G^{0.75}\, u_L \tag{23}$$

As also seen from Fig. 3, the volumetric mass transfer coefficient for carbon dioxide increases with both gas and liquid velocities.

## 3. Liquid Side Chemical Mass Transfer Coefficient

The results of the experiments carried out for the determination of the liquid side mass transfer coefficient with chemical reaction between absorbed carbon dioxide and sodium metaborate are presented in Fig. 4. The chemical mass transfer coefficient values obtained in this study are in very good agreement with similar studies on absorption of carbon dioxide in alkaline solutions with chemical reaction within the same gas and liquid velocity ranges [37,44].

The data given in this Fig. 4 were subjected to a regression analysis and the following equation was obtained:

$$(k_L a)_{CO_2} = 3.63u_G^{0.83}\, u_L^{0.11} \tag{24}$$

When the correlations developed for physical and chemical mass transfer coefficients are compared, while the effect of gas velocity is more or less the same, the relative effect of liquid velocity is smaller in case of chemical absorption. The exponent of the liquid velocity in Eq. (24) is much smaller than the one in Eq. (23) for the physical mass transfer coefficient: 0.11 vs 1. It is well known that for most industrial gas absorption applications, the main resistance to mass transfer lies at the liquid side. Any hydrodynamic effect such as increased turbulence in liquid due to increased liquid flow rate may help reduction in liquid side resistance. This becomes quite important for physical absorption. For chemical absorption, however, chemical reaction at the liquid side improves the absorption rate of solute profoundly and reduces the liquid side resistance to interfacial mass transfer appreciably. The effect of chemical reaction superimposes on the hydrodynamic effects because of liquid velocity and becomes the dominant contributor to the increase in mass transfer rate. This results in appreciable enhancement in mass transfer rate for chemical absorption.

Also note that the experiments were carried out with basic solution. The pH of the sodium metaborate solution used in the experiments was measured as 10.50 (±0.03) in the feed tank. The system was run continuously with respect to both phases and the exit liquid stream was collected in a different tank. For a short column like the one in the experiments, the amount of mass transfer and the amount of $CO_2$ absorbed was relatively small. The excess bulk
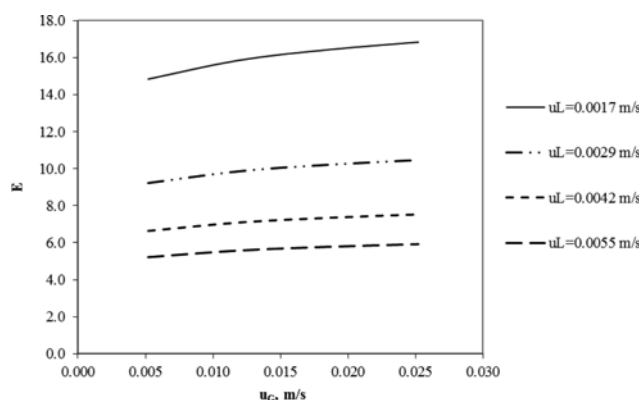
Fig. 5. Enhancement factors vs gas velocity.

concentration of metaborate did not change appreciably in single passage of liquid through the column. So, the acidification effect of $CO_2$ could be considered negligible in short once through systems. This in fact was also confirmed experimentally.

Eq. (21) together with Eqs. (23) and (24) were used to calculate the enhancement factor. The following equation was obtained and Fig. 5 was plotted using the enhancement factor values obtained.

$$E = 0.0775\, u_G^{0.08}\, u_L^{-0.89} \qquad (25)$$

The exponent of gas velocity in this equation is very small as expected. As the enhancement factor represents the increase in mass transfer due to the chemical reaction taking place in the liquid, it is reasonable to expect very small effect of gas velocity and relatively profound effect of liquid velocity. Also, the enhancement due to chemical reaction becomes more important at low liquid velocities. Mass transfer coefficient values at high liquid flow rates are already high because of hydrodynamic effects at high liquid velocities, so then the relative contribution of the reaction to the chemical mass transfer coefficient becomes less and less effective as liquid flow rate increases.

The enhancement factor values presented in Fig. 5 can help to understand the regime of chemical absorption taking place, i.e., fast pseudo-first-order reaction regime or transition regime or instantaneous regime. The reaction rate between carbon dioxide and sodium metaborate in the liquid can be expressed as below [18]:

$$r_C = k_r C_{CO_2}\, C_{SMB} \qquad (26)$$

The sodium metaborate concentration employed in the experiments for the determination of mass transfer coefficient was 4.5 wt-%. As the solubility of carbon dioxide in sodium metaborate solution of this specific concentration is about 34.50 mol/$m^3$ [45], one may safely assume that sodium metaborate was much in excess of carbon dioxide in the liquid. Thus, reaction rate can be expressed as pseudo first order reaction with respect to carbon dioxide.

$$r_C = r' C_{CO_2} \qquad (27)$$

where $k'$ is the overall rate constant and expressed as $k' = k_r C_{SMB}$.

The overall reaction rate constant was previously found as [18],

$$k' = 1.348 e^{\left(\frac{-18062}{RT}\right)} \qquad (28)$$

For fast pseudo first order reactions, the enhancement factor is equal to Hatta number:

$$E = Ha = \frac{\sqrt{k' D_{CO_2}}}{k_L^0} \qquad (29)$$

and it must lie within the interval between 2 and the infinite enhancement factor for istantaneous reactions, $E_\infty$ [16,39-42].

$$2 < Ha << E_\infty \qquad (30)$$

All the experimental values of the enhancement factors given in Fig. 5 are greater than two.

$E_\infty$, is the enhancement factor for instantaneous reaction which corresponds to maximum enhancement factor. It is dependent on the selected mass transfer model and for penetration theory it could be written as below [46,47]:

$$E_\infty = \left(1 + \frac{D_{SMB} C_{SMB}}{\gamma_{CO_2} D_{CO_2}^{SMB} C_{CO_2,\, i}}\right)\sqrt{\frac{D_{CO_2}^{SMB}}{D_{SMB}}} \qquad (31)$$

Here, $\gamma_{CO_2}$ is the stoichiometric coefficient. For the chemical system used, the parameters in Eq. (31) can be evaluated at 25 °C [48-56]. The diffusion coefficient of sodium metaborate in aqueous solutions ($D_{SMB}$) and the diffusion coefficient of carbon dioxide in sodium metaborate solution ($D_{CO_2}^{SMB}$) were calculated as $9.3497 \times 10^{-10}$ and $1.7516 \times 10^{-9}$ $m^2$/s, respectively. $E_\infty$ was then calculated as 14.07. Details of these calculations are given separately as the supplementary information. Recalling Eq. (31), this value of $E_\infty$ together with the experimental values given in Fig. 5 indicates that absorption of carbon dioxide by sodium metaborate solution does indeed take place essentially in the fast pseudo-first-order reaction regime.

Fig. 6 is drawn to show theoretically the variation of the enhancement factor for the chemical system used in this work with Hatta number. It is clear that the majority of data given in Fig. 5 essentially fall into the transition region and some approach to instantaneous region at low liquid velocities.

As noted, it has been reported that characteristic properties of bubble columns like gas holdup, interfacial area, physical mass transfer coefficient depend on the design of the column, type of the
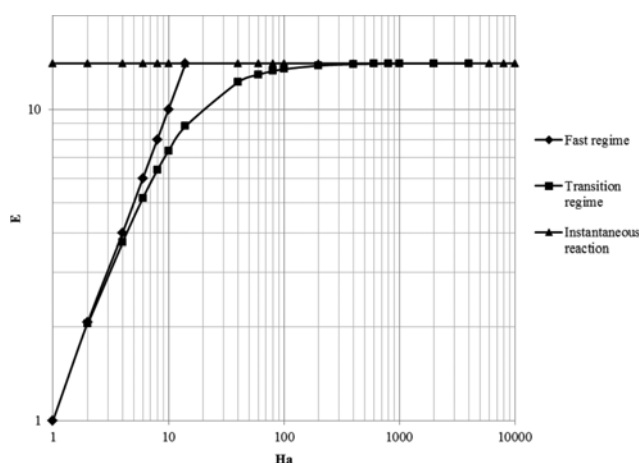


Fig. 6. Theoretical variation of the enhancement factor with Hatta number for the experimental system.

sparger, gas and liquid flow rates and gas-liquid system [43]. One has to consider all these as well as the diameter of the column before deciding on a correlation to use for these parameters. However, the enhancement factor is solely representing the effect of the specific reacting chemical system, and the enhancement factor is independent of hydrodynamic conditions of the liquid phase [57]. Thus, the equation for E (Eq. (25)) developed here can safely be used for carbon dioxide absorption into sodium metaborate solution in another column with a different column design and sparger if there is dependable information or a correlation for the estimation of the physical mass transfer coefficient for that column. More specifically, $k_L^0 a$ for the column of interest and E from Eq. (25) can be used to estimate $k_L a$ of the new contactor. This can then be used in the design or in calculations for rating the performance of the new column [58,59].

## CONCLUSIONS

We have shown that sodium metaborate can effectively be used to capture $CO_2$. For the bubble column used in the experiments, oxygen desorption method was used to find the physical mass transfer coefficient and a correlation was developed for it. Chemical mass transfer coefficient was also investigated in the system operated continuously with respect to both phases. To see the contribution of chemical reaction to the absorption, the enhancement factor was calculated and a correlation was developed. It was determined that absorption of carbon dioxide by sodium metaborate solution takes place essentially in the fast pseudo-first-order reaction regime.

## ACKNOWLEDGEMENTS

## NOMENCLATURE

a : interfacial area [m²/m³]
c : the total concentration at the liquid side [mol/m³]
$C_{CO_2}$ : carbon dioxide concentration [mol/m³]
$C_{SMB}$ : sodium metaborate concentration [mol/m³]
$D_{AB}$ : diffusivity of carbon dioxide [m²/s]
E : enhancement factor [-]
$E_\infty$ : infinite enhancement factor [-]
Ha : hatta number [-]
$k_L$ : liquid side physical mass transfer coefficient for carbon dioxide [m/s]
$k_r$ : reaction rate constant [m³/mol-s]
$k_x$ : volumetric mass transfer coefficient for carbon dioxide with fast chemical reaction [mol/m³-s]
$k_x^o$ : liquid side physical mass transfer coefficient [m/s]
$k'$ : pseudo first order reaction rate constant [1/s]
L : the liquid volumetric flow rate [m³/s]
$N_A$ : carbon dioxide molar flux [mol/m²-s]

$N_{CO_2}$ : average mass flux of carbon dioxide [mol/m²-s]
$r_c$ : reaction rate [mol/m³-s]
$S_c$ : cross-sectional area [m²]
$u_G$ : gas velocity [m/s]
$u_L$ : liquid velocity [m/s]
V : the liquid volume [m³]
W : the total rate of carbon dioxide absorption [mol/s]
$x_{bulk}$ : the liquid bulk composition [-]
$x_i$ : the interfacial composition at the liquid side in equilibrium [-]
$x_{in}$ : the inlet composition [-]
$x_{out}$ : the outlet composition [-]
$Z_T$ : the total liquid height [m]

**Greek Letters**

$\varepsilon_G$ : gas holdup [-]
$\varepsilon_L$ : liquid holdup [-]

## SUPPORTING INFORMATION

Additional information as noted in the text. This information is available via the Internet at http://www.springer.com/chemistry/journal/11814.

## REFERENCES

1. G. F. Versteeg, L. A. J. Van Dijck and W. P. M. Van Swaaij, *Chem. Eng. Commun.*, **144**, 113 (1996).
2. P. S. Kumar, J. A. Hogendoorn, G. F. Versteeg and P. H. M. Feron, *AIChE J.*, **49**, 203 (2003).
3. R. Dugas and G. Rochelle, *Energy Procedia*, **1**, 1163 (2009).
4. M. Edali, A. Aboudheir and R. Idem, *Int. J. Greenhouse Gas Control*, **3**, 550 (2009).
5. E. S. Hamborg, *Carbon dioxide removal processes by alkanolamines in aqueous organic solvents*, Ph.D. Thesis, University of Groningen, Enschede (2011).
6. J. H. Meldon and M. A. Morales-Cabrera, *Chem. Eng. J.*, **171**, 753 (2011).
7. A. L. Kohl and R. Nielsen, *Gas Purification*, 5th Ed., Gulf Publishing Co., Houston (1997).
8. U. E. Aronu, H. F. Svendsen, K. A. Hoff and O. Juliussen, *Energy Procedia*, **1**, 1051 (2009).
9. U. E. Aronu, H. F. Svendsen and K. A. Hoff, *Int. J. Greenhouse Gas Control*, **4**, 771 (2010).
10. G. S. Goff and G. T. Rochell, *Ind. Eng. Chem. Res.*, **43**, 6400 (2004).
11. A. F. Portugal, P. W. J. Derks, G. F. Versteeg, F. D. Magalhães and A. Mendes, *Chem. Eng. Sci.*, **62**, 6534 (2007).
12. P. M. M. Blauwhoff, G. F. Versteeg and W. P. M. Van Swaaij, *Chem. Eng. Sci.*, **38**, 1411 (1983).
13. J. T. Yeh, K. P. Resnik, K. Rygle and H. W. Pennline, *Fuel Process. Technol.*, **86**, 1533 (2005).
14. P. W. J. Derks and G. F. Versteeg, *Energy Procedia*, **1**, 1139 (2009).
15. V. Telikapelli, F. Kozak, J. F. Leandri, B. Sherrick, J. Black, D. Muraskin, M. Cage, M. Hammond and G. Spitznogle, CCS with the Alstom chilled ammonia process development program - field pilot results. *Presented at Greenhouse Gas Technology 10 (GHGT*

10), Amsterdam (2010).

16. V. Darde, W. J. M. Van Well, P. L. Fosboel, E. H. Stenby and K. Thomsen, *Int. J. Greenhouse Gas Control*, **5**, 1149 (2011).

17. J. Liu, S. Wang, G. Qi, B. Zhao and C. Chen, *Energy Procedia*, **4**, 525 (2011).

18. D. Uysal, O. M. Dogan and B. Z. Uysal, *Int. J. Chem. Kinet.*, **49**, 377 (2017).

19. M. T. Ityokumbul, N. Kosaric and W. Bulani, *Chem. Eng. J.*, **53**, 167 (1994).

20. B. Haut, V. Halloin, T. Cartage and A. Cockx, *Chem. Eng. Sci.*, **59**, 5687 (2004).

21. N. Kantarci, F. Borak and K. O. Ulgen, *Process Biochem.*, **40**, 2263 (2005).

22. H. A. Jakobsen, I. Bourg, K. W. Hjarbo and H. F. Svendsen, *Parallel Computational Fluid Dynamics - Trends and Applications*, Elsevier, New York (2001).

23. H. Dhaouadi, S. Poncin, J. M. Hornut and N. Midoux, *Chem. Eng. Process. Process Intensif.*, **47**, 548 (2008).

24. E. Álvarez, D. Gómez-Díaz, J. M. Navaza and B. Sanjurjo, *Chem. Eng. J.*, **137**, 251 (2008).

25. P. Harriot, *Chemical Reactor Design*, Marcel Dekker, New York (2002).

26. S. Degaleesan, M. Dudukovic and Y. Pan, *AIChE J.*, **47**, 1913 (2001).

27. C. L. Hyndman, F. Larachi and C. Guy, *Chem. Eng. Sci.*, **52**, 63 (1997).

28. H. F. Bach and T. Pilhofer, *Ger. Chem. Eng.*, **1**, 270 (1978).

29. U. Oels, J. Lucke, R. Buchholz and K. Schugerl, *Ger. Chem. Eng.*, **1**, 115 (1978).

30. R. Krishna, P. M. Wilkinson and L. L. Van Dierendonck, *Chem. Eng. Sci.*, **46**, 2491 (1991).

31. F. Yamashita and H. Inoue, *J. Chem. Eng. Jpn.*, **8**, 444 (1975).

32. R. M. Adams and R. M. Boron, *Metallo-boron Compounds and Boranes*, Wiley, USA (1964).

33. J. O. Edwards, G. C. Morrison, V. F. Ross and J. W. Schultz, *J. Am. Chem. Soc.*, **77**, 266 (1955).

34. W. D. Deckwer, Y. Louisi, A. Zaidi and M. Ralek, *Ind. Eng. Chem. Process Des. Dev.*, **19**, 699 (1980).

35. R. H. Perry and D. W. Green, *Perry's Chemical Engineers' Handbook*, 8th Ed., McGraw Hill, New York (2008).

36. A. H. G. Cents, F. T. de Bruijn, D. W. F. Brilman and G. F. Versteeg, *Chem. Eng. Sci.*, **60**, 5809 (2005).

37. P. C. Chen, W. Shi, R. Du and V. Chen, *Ind. Eng. Chem. Res.*, **47**,

6336 (2008).

38. L. S. Fan, *Gas-Liquid-Solid Fluidization Engineering*, Butterworths, New York (1989).

39. Y. T. Shah, B. G. Kelkar, S. P. Godbole and W. D. Deckwer, *AIChE J.*, **28**, 353 (1982).

40. J. B. Joshi and M. M. Sharma, *Trans. Inst. Chem. Eng.*, **57**, 244 (1979).

41. Y. Kawase and M. Moo-Young, *Chem. Eng. Res. Des.*, **65**, 121 (1987).

42. X. Luo, D. J. Lee, R. Lau, G. Yang and L. S. Fan, *Chem. Eng. Process*, **45**, 665 (1999).

43. P. Zehner and M. Kraume, *Bubble Columns in Ullmann's Encyclopedia of Industrial Chemistry*, Wiley VCH Verlag GmbH &Co. KGaA, Weinheim (2000).

44. E. Sada, H. Kumazawa, C. Lee and N. Fujiwara, *Ind. Chem. Eng. Process Des. Dev.*, **24**, 255 (1985).

45. S. Weisenberg and A. Schumpe, *AIChE J.*, **42**, 298 (1996).

46. P. V. Danckwerts, *Gas-liquid Reactions*, McGraw-Hill, New York (1970).

47. R. Higbie, *Trans. Am. Ins. Chem. Eng.*, **31**, 365 (1935).

48. Y. Zhou, C. Fang, Y. Fang and F. Zhu, *Chin. J. Chem. Eng.*, **21**, 1048 (2013).

49. J. G. Speight, *Lange's Handbook of Chemistry*, 16th Ed., McGraw-Hill, New York (2005).

50. B. E. Poling, J. M. Prausnitz and J. P. O'Connell, *The Properties of Gases and Liquids*, 5th Ed., McGraw-Hill, New York (2004).

51. G. F. Versteeg and W. P. M. Van Swaaij, *J. Chem. Eng. Data*, **33**, 29 (1988).

52. C. R. Cloutier, A. Alfantazi and E. Gyenge, *Adv. Mater. Res.*, **15-17**, 267 (2007).

53. C. Hermann and A. Schumpe, *AIChE J.*, **42**, 298 (1996).

54. A. Schumpe and W. D. Deckwer, *Biotechnol. Bioeng.*, **21**, 1075 (1979).

55. S. E. Licht and R. H. Weiland, Density and physical solubility of carbon dioxide in partial loaded solution of MEA, DEA and MDEA and their blends, *Presented at the Spring National Meeting. American Institute of Chemical Engineers*, Paper no.57f, Houston, Texas (1989).

56. H. Dang and G. T. Rochelle, *Sep. Sci. Technol.*, **38**, 337 (2003).

57. G. Astarita, *Mass Transfer with Chemical Reactions*, Elsevier, Amsterdam (1967).

58. K. T. Putta, F. A. Tobiesen, H. F. Svendsen and H. K. Knuutila, *Appl. Energy*, **206**, 765 (2017).

59. M. Krau and R. Rzehak, *Chem. Eng. Sci.*, **166**, 193 (2017).

# Supporting Information

# Mass transfer enhancement factor for chemical absorption of carbon dioxide into sodium metaborate solution

**Duygu Uysal Zıraman[†], Özkan Murat Doğan, and Bekir Zühtü Uysal**

Department of Chemical Engineering and Clean Energy Research and Application Center (CERAC-TEMENAR),
Gazi University, Maltepe, Ankara, 06570, Turkey

The diffusion coefficient of carbon dioxide in sodium metaborate solution can be calculated with the correlation given below [14].

$$D_{CO_2}^{SMB} = D_{CO_2}^{H_2O}\left(\frac{\mu_{H_2O}}{\mu_{SMB}}\right)^{0.8}$$

According to the given relation, the diffusion coefficient of carbon dioxide in water should be calculated. This can be achieved by using the correlation given below [51].

$$D_{CO_2}^{H_2O} = 2.35 \times 10^{-6} e^{\left(-\frac{2116}{T(K)}\right)}$$

The experiments were done at 25 °C, so the value of this diffusion coefficient was as follow.

$$D_{CO_2}^{H_2O} = 1.94463 \times 10^{-9} \text{ m}^2/\text{s}$$

The viscosity of water was calculated with the following correlation.

$$\mu_{H_2O} = 1.18 \times 10^{-6} e^{16400/RT}$$

At 25 °C, this value is $\mu_{H_2O} = 8.815 \times 10^{-4}$ kg/m-s.

The viscosity of sodium metaborate at 25 °C is $1.00457 \times 10^{-3}$ kg/m-s [48].

With these values, the diffusion coefficient of carbon dioxide in sodium metaborate solution ($D_{CO_2}^{SMB}$) was calculated as $1.7516 \times 10^{-9}$ m²/s.

The diffusion coefficient of sodium metaborate in aqueous solutions was calculated with the correlation given below [14].

$$D_{SMB}\mu_{SMB}^{0.6} = D_{SMB}^0(\mu^0)^{0.6}$$

Here, $D_{SMB}^0$ is the diffusion coefficient of sodium metaborate in infinitely dilute solution and $\mu^0$ is the viscosity of it, which can be accepted as the viscosity of water at that temperature. In order to calculate $D_{SMB}^0$ Nernst equation was used that is given below [50].

$$D_{SMB}^0 = \frac{RT[(1/z_+) + (1/z_-)]}{F^2[(1/\lambda_+^0) + (1/\lambda_-^0)]}$$

Here, $z_+$ and $z_-$ are the valencies of cation and anion, respectively. F is the Faraday constant, which is 96,500 °C/mol. $\lambda_+^0$ and $\lambda_-^0$ are the ionic molar conductivities of ions and the values of them are 50.11 and 30.59 S·cm²/mol, respectively [52].

With all of these values given, the diffusion coefficient of sodium metaborate in aqueous solutions was calculated as $9.3497 \times 10^{-10}$ m²/s.

To calculate the solubility of carbon dioxide in sodium metaborate solution, Henry's law constant is needed. In order to calculate the Henry's law constant, Setschenow equation is used [53].

$$\log\left(\frac{H_{CO_2}^{H_2O}}{H_{CO_2}^{SMB}}\right) = KC_s$$

Here, $H_{CO_2}^{H_2O}$ is the Henry's law constant of carbon dioxide in water. K is the Setschenow constant. This constant is dependent on gas and salt solution used and can be calculated with the equation given below [54].

$$K = \Sigma(h_i + h_G)n_i$$

Here, $h_i$ and $h_G$ are the specific parameters of ions and gas, respectively. The values of these parameters are −0.0172, 0.1762 and 0.0726 m³/kmol for $h_G$, $h_+$ and $h_-$, respectively (the specific ion parameter for borate ion is adapted from nitrite ion due to the similarity as recommended in the literature) [45,46].

The Henry's law constant of carbon dioxide in water was calculated with the correlation given below [55,56].

$$H_{CO_2}^{H_2O} = 100e^{\left(-\frac{2625}{T} + 12.2\right)}$$

With all of the values and correlations given, the Henry's law constant of carbon dioxide in sodium metaborate solution used in the experiments was calculated as 2321.171 Pa-m³/mol. Thus the interfacial concentration of carbon dioxide, $C_{CO_2,i}$, was calculated as 39.345 mol/m³.